



HAL
open science

Evaluation of damage in neutron irradiated boron carbide

Dominique Gosset, Patrick Herter, Vianney Motte

► **To cite this version:**

Dominique Gosset, Patrick Herter, Vianney Motte. Evaluation of damage in neutron irradiated boron carbide. Nuclear Instruments and Methods in Physics Research Section B: Beam Interactions with Materials and Atoms, 2018, 434, pp.66-72. 10.1016/j.nimb.2018.08.021 . cea-02430090

HAL Id: cea-02430090

<https://cea.hal.science/cea-02430090>

Submitted on 7 Jan 2020

HAL is a multi-disciplinary open access archive for the deposit and dissemination of scientific research documents, whether they are published or not. The documents may come from teaching and research institutions in France or abroad, or from public or private research centers.

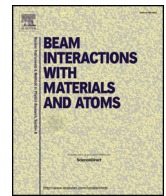
L'archive ouverte pluridisciplinaire **HAL**, est destinée au dépôt et à la diffusion de documents scientifiques de niveau recherche, publiés ou non, émanant des établissements d'enseignement et de recherche français ou étrangers, des laboratoires publics ou privés.



ELSEVIER

Contents lists available at ScienceDirect

Nuclear Inst. and Methods in Physics Research B

journal homepage: www.elsevier.com/locate/nimb

Evaluation of damage in neutron irradiated boron carbide

Dominique Gosset^{a,*}, Patrick Herter^b, Vianney Motte^a^a CEA, Université Paris-Saclay, DEN-SRMA, F-91191 Gif sur Yvette, France^b CEA, Université Paris-Saclay, DEN-DISN-VALO, F-91191 Gif sur Yvette Cedex, France

ARTICLE INFO

Keywords:

Neutron absorber
 Damage rate
 Boron carbide
 Ion implantation simulation

ABSTRACT

When irradiated in a reactor, neutron absorber materials undergo two different damages induced, first, by the elastic scattering of neutrons; second by the neutron absorption reactions. In boron carbide irradiated in a fast neutron flux, neutron scattering and the slowing-down of He and Li arising from the (n,α) absorption reaction both lead to the displacement of B and C atoms which energy ranges up to a few MeV. Simulating the neutron damage by ion irradiation requires the calculation of the damage produced in both cases. In this paper we propose an estimation of the actual defect production rate resulting from the fast neutron irradiation. For this, we first estimate the energy spectra of both the primary knocked-on atoms and atoms created by the absorption reactions, here in a Phenix-like neutron spectrum. We then deduce from SRIM calculations the actual energy distribution of all the atoms displaced along the displacements cascades induced by those primary projectiles. At last, we obtain an estimation of the number of displaced atoms per produced helium, about 305, most of them resulting from neutron scattering. This is far from a Kinchin-Pease or NRT estimation, of the order of several thousands, this arising from the fact that most of the energy is dissipated through electronic interactions. Such results are then used in order to perform ion irradiations aiming at a realistic simulation of synergetic effects of helium implantation and damage production.

1. Introduction

Ion implantations are widely used to simulate the damage and the composition change arising in materials irradiated in nuclear plants [1,2]. However, some parameters can hardly be accounted for; for example, a reactor irradiation most often last up to a few years to be compared to a few hours for an ion implantation, this making kinetics effects difficult to handle. Another parameter is the way the energy is dissipated into the material. The slowing-down of the particles happens according to two different processes [3]; either an interaction with the electrons (electronic slowing-down, associated with the electronic stopping power, Se) or with the nuclei (nuclear stopping power, Sn). The former is of low consequences in metals (energy dissipation in the electron sea) but can induce important effects in insulators or semiconductors [4]. Moreover, in some conditions, nuclear reactions happen (fuel, neutron absorber, tritium blankets in ITER, spallation sources...). In those cases, first the composition of the material is modified, but second the reaction products can be energetic enough to produce defects.

We are here interested in the behavior of helium in boron carbide. Boron carbide is widely used as a neutron absorber, either in thermal or fast neutron flux [5]. The main absorption reaction is the $^{10}\text{B}(n,\alpha)^7\text{Li}$

one. In fast neutron reactor, helium can be produced in large quantities, about $10^{22}/\text{cm}^3$ (i.e. concentration about 0.1), leading to swelling and cracking of the material. ^4He and ^7Li are emitted with energies in the MeV range (mass defect of the main absorption reaction). Owing to the low atomic mass of the constituents of the material, they can then produce structural defects. On the other hand, in a fast neutron flux, the primary knocked-on atoms (pka) produced by neutron scattering have an energy spectrum up to a few MeV, high enough to displace the atoms of the material. In both cases, neutron absorption or scattering, the nuclei emerging from the reaction are light ones (B, C, Li, He). They will slow-down in a matrix also constituted of light nuclei. In that case, it is known that most of the pka energy is dissipated by electronic interaction. However, some atomic displacements arise, mostly at the end of the ion paths. The questions which arise are then the ratio of produced helium to the total number of displaced atoms, the way energy is dissipated, and the consequence of the damage on the kinetics of helium, e.g. nucleation and growth of clusters.

Simulating the behavior of helium in boron carbide with ion implantations then leads to wonder if the associated damage in reactor can be reproduced as well as the gas concentration. For that, it is necessary to perform ion irradiations which parameters such as the damage to helium concentration ratio or the Se/Sn ratio are precisely known and

* Corresponding author.

E-mail addresses: dominique.gosset@cea.fr (D. Gosset), patrick.herter@cea.fr (P. Herter), viamotte@hotmail.fr (V. Motte).<https://doi.org/10.1016/j.nimb.2018.08.021>

Received 20 November 2017; Received in revised form 7 August 2018; Accepted 17 August 2018

Available online 25 August 2018

0168-583X/ © 2018 Elsevier B.V. All rights reserved.

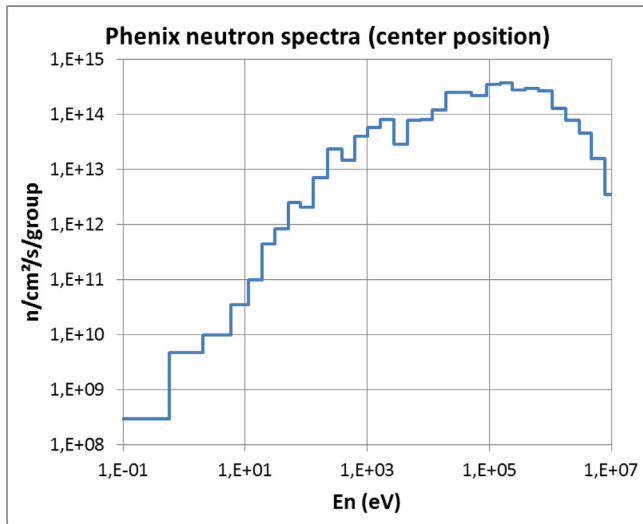


Fig. 1. Neutron spectrum at the center of the late French Phenix LMFBR [10].

representative. Such estimations can be done e.g. with tools such as SRIM [6]. But the comparison with the reactor conditions requires making this estimation with the actual reactor parameters. The available data are the material characteristics, the neutron flux in the reactor and the interaction cross sections. Here, we detail the route we have followed from those nuclear data to the atoms displacement rate (obtaining the helium production rate is straightforward, by convoluting the neutron spectrum and the absorption cross section). The first step is calculating the so-called primary damage spectrum [7–9], i.e. the energy distribution of the pka and of the created atoms by the absorption reactions. We then use the SRIM software to estimate the number of displaced atoms as a function of the pka's energy and the way energy is dissipated. At last, those results allow us to estimate the helium to atomic displacements ratio and the electronic stopping power range.

2. Data

We consider a neutron spectrum equivalent to the one in the center of the late French Phenix LMFBR (sodium cooled fast neutron reactor) [10]. The spectrum is divided in 36 groups (Fig. 1). The total flux is about $3.10^{15} \text{ n.cm}^{-2}.\text{s}^{-1}$.

The neutron interaction cross sections (neutron scattering and absorption) are taken from the ENDF data base [11]: Figs. 2 and 3. For the absorption reactions, we consider only the $^{10}\text{B}(n,\alpha)^7\text{Li}$ one. We then neglect the $^{10}\text{B}(n,2\alpha)^3\text{H}$ reaction. As a matter, the cross section for this reaction is about 10^{-6} lower than the (n,α) one, excepted in the fast neutron range (where it is rather poorly known [12]), where the neutron flux significantly decreases, leading to a production rate about one thousand lower than the (n,α) one. Second, it has a lower mass defect, about 0.23 MeV to be compared to about 2.8 MeV for the (n,α) reaction, leading to a much lower energy of the pka's. Excepted in the fast neutron range, the (n,α) absorption cross section varies as $\sigma = 611/\sqrt{E}$ (σ in barn, E in eV). Convoluting the neutron spectrum and the (n,α) absorption cross section leads to the helium production rate:

$$\tau_{\text{He}} = 4,01 \times 10^{-9} \text{ at}^{-1}.\text{s}^{-1}$$

where 'at' stands for an equivalent boron carbide atom (initially full density $\text{B}_{0.8}\text{C}_{0.2}$, 48% ^{10}B enriched, $10^{22}/\text{cm}^3$ burnup: see here under).

In order to have a good estimation of the damage on all the atoms, including the neutron capture products, we consider a highly irradiated boron carbide sample. We have chosen a $10^{22}.\text{cm}^{-3}$ capture density (most often called burnup). The boron concentration in non-irradiated B_4C boron carbide is about $1.1 \times 10^{23}.\text{cm}^{-3}$. As a result, the mean atomic composition of the irradiated material is taken as $\text{B}_{0.72}\text{C}_{0.2}\text{He}_{0.08}\text{Li}_{0.08}$.

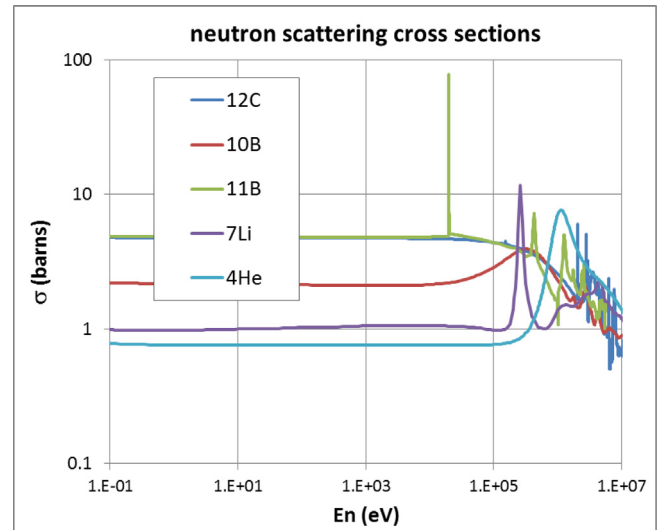


Fig. 2. Neutron scattering cross sections on the isotopes to be considered, ^{10}B , ^{11}B , ^{12}C , ^7Li , ^4He , from [11].

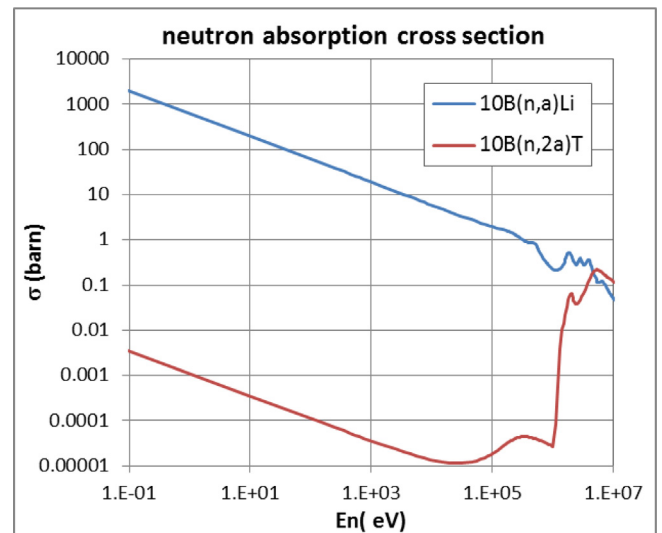


Fig. 3. Neutron absorption cross section for the $^{10}\text{B}(n,\alpha)^7\text{Li}$ and $^{10}\text{B}(n,2\alpha)^3\text{H}$ reactions, from [11].

The initial ^{10}B enrichment of boron is taken as 48%, which reduces to 39% for a $10^{22}.\text{cm}^{-3}$ burnup.

Estimating the atom displacement rates requires the knowledge of the displacement energy threshold (TDE) for all the atoms of the material. Here we consider only mean values. For B and C, we have considered the values proposed in SRIM, which are coherent with the estimations performed by Zuppiroli et al. [13]. For He, we have used a most recent estimation of the thermal diffusion energy [14]. For Li, we have used an arbitrary, intermediate value: the only available value is for lithium aluminate, about 22 eV, i.e. in a quite different electronic environment with strong ionic bondings we have supposed higher than in B_4C [15]. Now, on a formal point of view, this value is of low importance: Li emitted with energy close to the TDE is unable to displace B or C and is of low efficiency on He. The values are then the followings:

- B: 25 eV
- C: 28 eV
- He: 2 eV
- Li: 15 eV

3. Primary damage spectra

The primary damage spectra are the sum of two components:

- The pka arising from the ballistic scattering of the neutron,
- The atoms emerging from the neutron absorption reactions.

The first term requires considering the kinematics of the neutron – atom scattering reaction. The second one is on a first step given by the energy taken by He and Li but has to take into account the energy of the impinging neutron. In both cases, we consider for simplicity the neutron – nuclei reactions cross sections are isotropic.

3.1. Neutron – atom scattering reaction

From classical results of kinematics, a pka of mass M elastically hit by a neutron of mass m and kinetic energy E will get a kinetic energy E' which probability density function $f(E',E)$ is uniform from 0 to a maximum energy given by:

$$E'_{max} = \gamma E$$

$$\text{with } \gamma = \frac{4Mm}{(M+m)^2}$$

Integrating the contribution of all the neutrons through the whole spectrum ϕ with σ_{elast} the elastic cross section leads to the number of pka per second and pka energy unit given by:

$$\frac{dN'}{dE'} = \frac{1}{\gamma} \int_{E \geq E'/\gamma} \phi(E) \sigma_{elast}(E) \frac{dE}{E} \quad (\text{at}^{-1} \cdot \text{s}^{-1} \cdot \text{eV}^{-1}) \quad (1)$$

3.2. Energy spectra of produced He and Li

The He pka kinetic energy E' resulting from fission induced by a neutron absorption of ^{10}B does not only depend on the fission energy but also on the impacting neutron kinetic energy E . In the center of mass referential, He is emitted with about 1.8 MeV and Li with 1.0 MeV. Those energies have to be evaluated to take into account the energy of the impinging neutron and its space distribution. We assume that the loss of mass due to the fission is negligible. Conservation laws of energy and momentum lead to formulas depending both on the masses of the parent isotope ^{10}B (M) and the fission products ^4He (m_{He}) and ^7Li (m_{Li}). Let the two characteristic energies be:

$E'_0 = E_{fission} \frac{m_{Li}}{m_{He} + m_{Li}}$ (He energy resulting from a neutron of null energy, equal to the value in the center of mass referential)

$E'_0 = E_{fission} \frac{m_{Li}}{m_{He}} \frac{M+m}{m}$ (neutron energy leading to a He staying at rest after its creation)

The kinetic energy E' of the created He may be expressed in the following form:

$$E' = E'_0 \left[1 + \frac{E}{E'_0} + 2 \sqrt{\frac{E}{E'_0}} \cos(2\pi X) \right]$$

where X is a uniform random number between -1 and $+1$ (due to the isotropic recoil direction in the mass center coordinates), which leads to a probability density function of the pka energy E' given by the formula:

$$f(E', E) = \frac{1}{4E'_0 \sqrt{\frac{E}{E'_0}}} \quad (2)$$

where E' ranges between $E'_0 \left(\sqrt{\frac{E}{E'_0}} - 1 \right)^2$ and $E'_0 \left(\sqrt{\frac{E}{E'_0}} + 1 \right)^2$

For a whole neutron spectrum ϕ and an absorption cross section σ_{abs} this leads to a number of He created per second and He energy unit given by

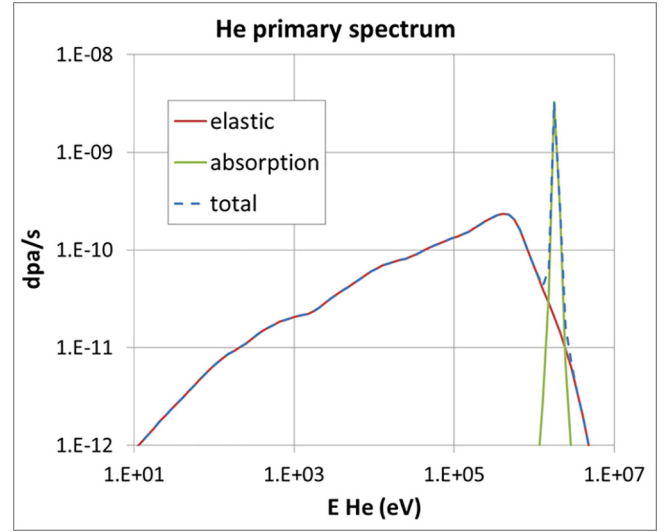


Fig. 4. Primary spectrum for He, showing the contribution of the neutron scattering (elastic) and absorption (for a He content = $10^{22}/\text{cm}^3$).

$$\frac{dN'}{dE'} = \int_{E'_0 \left(\sqrt{\frac{E'}{E'_0}} - 1 \right)^2}^{E'_0 \left(\sqrt{\frac{E'}{E'_0}} + 1 \right)^2} \frac{\phi(E) \sigma_{abs}(E) dE}{4E'_0 \sqrt{\frac{E'}{E'_0}}} \quad (\text{at}^{-1} \cdot \text{s}^{-1} \cdot \text{eV}^{-1}) \quad (3)$$

Similar formulas are derived for Li.

Calculations are performed by a numerical method with a log scale for the energies (lethargy units).

4. Results

4.1. Primary spectra

The primary spectra for the different isotopes are reported on Figs. 4 and 5. They span from the eV range (depending on the threshold displacement energies) to the MeV range (depending on the atom mass over neutron mass ratio). In the case of helium (lithium is similar), Fig. 4 clearly shows the two components: displacements by the neutrons (“elastic” component) and energy distribution of He produced by the absorption reaction (“fission” component). The latter is proportional to He concentration and is here calculated for a He concentration of $10^{22}/\text{cm}^3$. Taking into account the energy distribution of the absorbed neutron, He atoms (resp. Li) are emitted with an energy distribution spanning over several energy groups of the neutron spectrum. On Fig. 5, the curves are limited on the low energy side by the threshold displacement energies. The steep decrease of the curves on the high energy side justifies not having taken into account the $^{10}\text{B}(n,2\alpha)\text{T}$ reaction. Integrating the primary spectra curves shows that most of the pkas have energy above 10 keV (Fig. 6).

This calculation can then be used to estimate the pka formation rates (Table 1).

4.2. Displacements induced by pka's and created atoms

After calculating the primary spectra, it is necessary to estimate the number of displaced atoms of each species as a function of the pka's energy. For that, we used the SRIM program in the “full cascade” mode [6]. This allows an estimation of the number of the displaced atoms by a given incident ion, including the sub-cascades, and of the way energy is dissipated. Calculations are performed with 5000 ions in each case. The material is simulated with the composition we detailed above, then with an equivalent boron atom with a 10.6 atom mass. For the sake of

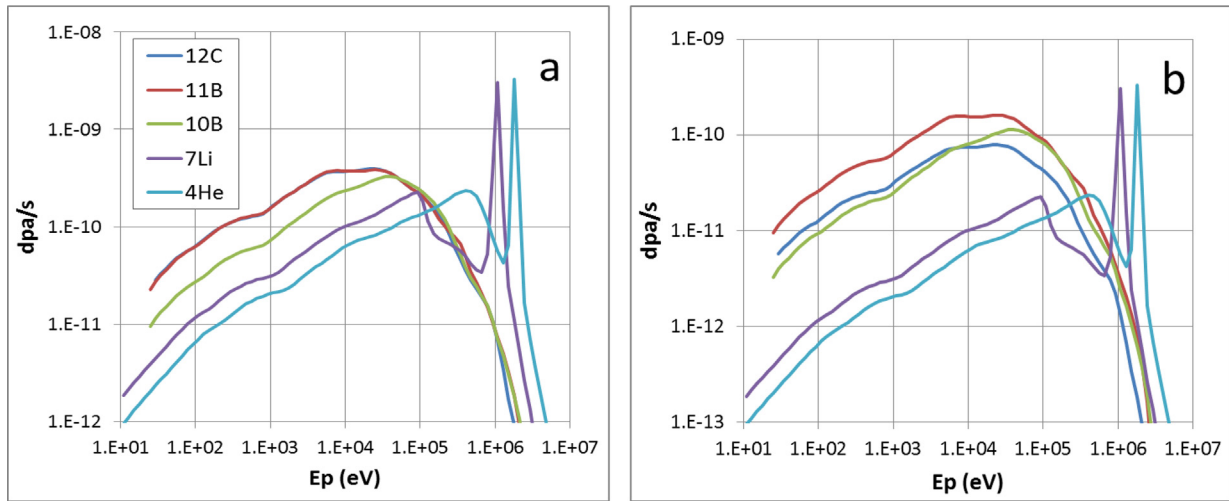


Fig. 5. Primary spectra for all the isotopes in irradiated B_4C , for an initial ^{10}B enrichment = 48% and a $10^{22}/cm^3$ burnup. a: per isotope; ^{12}C and ^{11}B show very similar profiles. b: reported to an equivalent B_4C atom with $10^{22} (n,\alpha)/cm^3$.

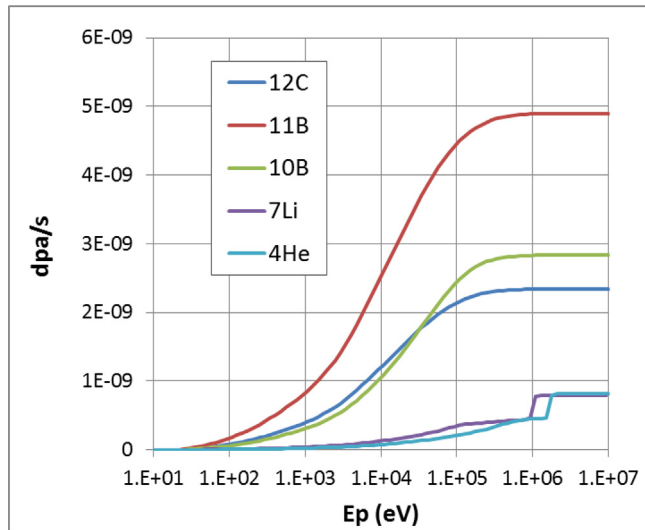


Fig. 6. Integral weighed primary spectra for B_4C ($10^{22}/cm^3$ burnup) in a Phenix-like neutron spectrum. Most of the pka's have energy above 10 keV. The steps at about 1 MeV on the He and Li curves correspond to the (n,α) contribution.

Table 1

pka formation rate for all the isotopes in irradiated boron carbide for an equivalent B_4C atom (^{10}B enrichment = 39%, He = Li = $10^{22}.cm^{-3}$).

Pka. s^{-1} ($\times 10^9$)	^{12}C	^{11}B	^{10}B	7Li	4He
	2.34	4.90	2.83	0.79	0.82

simplicity, those calculations have been performed on a few pka energies evenly distributed along a pka energy logarithmic range from 100 eV to 4 MeV.

On Fig. 7 we reported the results of the SRIM calculation in the case of a ^{12}C ion with a 1 MeV initial energy. As emphasized above, it appears most of the energy is dissipated via electronic interactions: Fig. 8. Atoms displacements occur mainly at the end of the C path or for a C primary atom energy lower than 10 keV. Due to the mass ratio and threshold displacement energies, the relative displacement yield of helium appears much higher than the B or C ones.

In the case of low-energy pka's, SRIM leads to a non-negligible number of back-scattered atoms. In the case of a reactor irradiation,

those atoms correspond to ones emitted in a backward direction. Their energy can however be high enough to produce defects in a bulk material. To take into account this contribution, we have extrapolated the 'range' profiles as calculated by SRIM towards the negative paths, assuming Gaussian-like profiles (Fig. 9). The displacements rates have then been increased in the surface of the Gaussian over surface of the range curve ratio.

The results we obtained for each impinging atom are reported on Fig. 10. Here again a high mobility is observed on He, due to its low atom mass. Polynomial fittings of the results have then been performed. Those polynomials are then convoluted with the primary spectra, this leading to the total number of displaced atoms: Table 2.

As mentioned in Section 2, the helium production rate is about $4.01.10^{-9} s^{-1}$ per equivalent B_4C atom. From those results, we deduce the number of displaced B and C atoms per produced helium (i.e. $(973 + 252)/4.01$) is about 305, and 280 when neglecting the damage induced by the slowing down of He and Li produced in the (n,α) reactions. This second contribution is then less than 10% (it is worth noting that this contribution would become the main one in a thermal neutron flux). This is far from an estimation in the Kinchin-Pease or NRT (Norgett-Robinson-Torrens) approximations [16,17] which lead to a displaced atoms over produced helium ratio of several thousands (at first order, the pka yield is evaluated by the pka energy divided by twice the threshold displacement energy). Again, this is due to the fact that most of the energy is dissipated through electronic processes.

Regarding the electronic energy losses, their intensity has to be examined. As a matter, depending on this intensity, this contribution can either produce damage (e.g., tracks in insulators), heal the material [18] or have no noteworthy effect. Here, the electronic stopping power is at maximum $160 eV.\text{\AA}^{-1}$ for C, $125 eV.\text{\AA}^{-1}$ for B, $75 eV.\text{\AA}^{-1}$ for Li and $45 eV.\text{\AA}^{-1}$ for He for the highest primary atom energy. This can certainly not lead to damage (the usual threshold value for producing damage is about or higher than $1 keV.\text{\AA}^{-1}$) but could possibly allow a low healing of some defects. This could be studied by tuning the Se over Sn ratio at constant Sn value: this could be achieved by performing dual beam experiments (cf. infra).

4.3. Application

We have then evaluated the damage produced by different ions of different energy (see [19] for the choice of some ions) to estimate the possibility of reproducing the damage evaluated in the previous section (Table 3.).

From the previous estimations, it appears that reproducing the

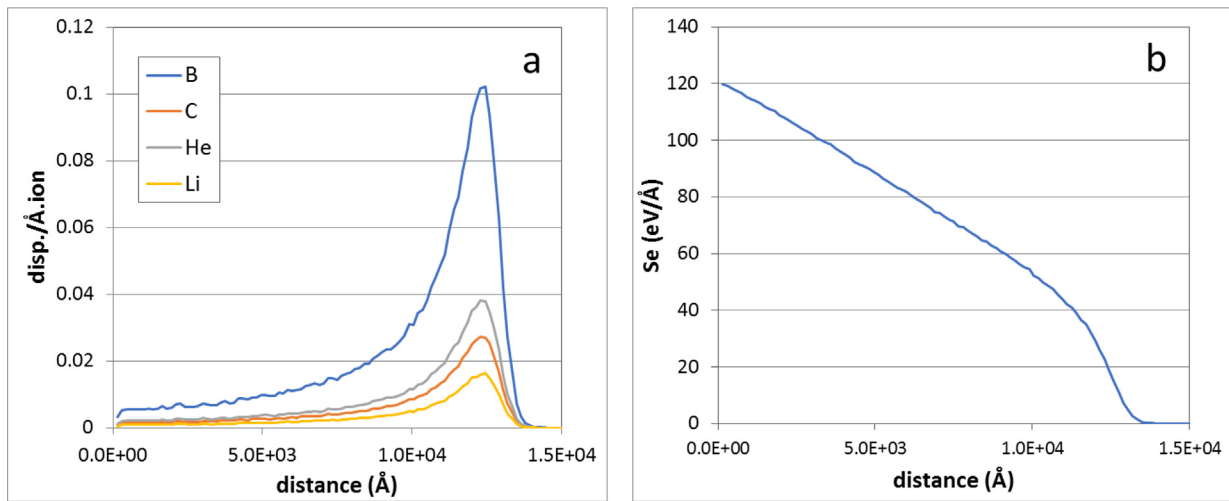


Fig. 7. SRIM calculation for a ^{12}C atom with initial energy 1 MeV in B_4C with $10^{22}/\text{cm}^3$ He and Li. a: number of displaced atoms along the ion range. b: electronic losses.

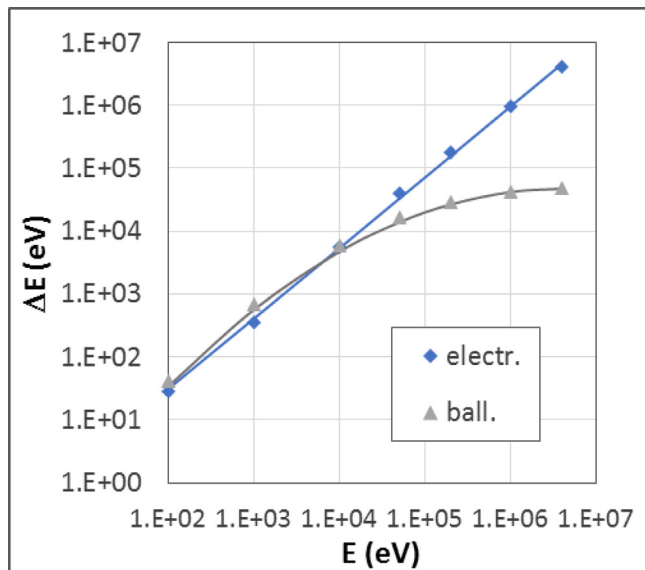


Fig. 8. Partition of the energy losses for C atoms in 'B4C' as a function of C initial energy. Electr.: electronic losses. Ball.: ballistic losses.

damage arising in a fast neutron reactor with ion irradiation in boron carbide requires a high ballistic component together with low electronic losses. This can be achieved by using slow heavy ions. But in this case, the ion range is very short and the damage zone is strongly superimposed to the implantation one, which is not desirable. This is of course no longer acceptable if helium has to be implanted in the damage zone. An acceptable compromise is to use heavy ions with intermediate energy (a few MeV): in that case, the ballistic damage can be made realistic and the electronic slowing down is a bit too high but still far from the range where specific damage such as ion tracks appear [19]. In the case of dual-beam experiments, it is worth noting that we are interested in creating a realistic damage in the zone where helium is implanted. We then only consider the atom displacements in the damage region of the slowing-down of the heavy ions, not in the stopping region. As a consequence, the structure of the damage, i.e. the space distribution of the displaced atoms does not include all the cascades. This is an important point to consider since it is known that the largest cascades are produced at the end of the heavy ion course: in the damage region, most of displacements arise from small cascades which structure is rather close to those created by the stopping of the matrix

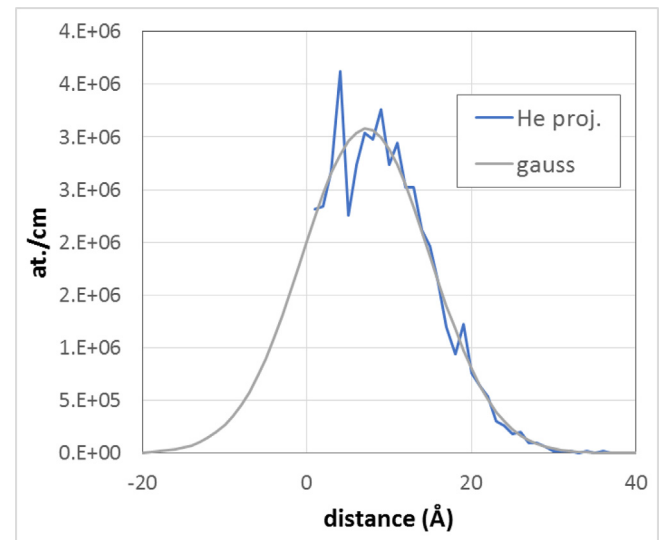


Fig. 9. Range of 100 eV ^4He in B_4C (with $10^{22}/\text{cm}^3$ burnup). The back-scattered atoms yield is estimated by extrapolating a Gaussian profile fitted on the helium distribution into the material.

atoms in the reactor, i.e. B and C with energy up to a few MeV.

Preliminary tests have been performed [20,21] aiming at reproducing the helium to damage ratio together with a significant helium concentration. We have irradiated a high density boron carbide sample with a dual beam on the Jannus-Saclay facility [22]:

- $10^{16}/\text{cm}^2$, 500 keV He (peak at 1.2 μm depth, FWHM $\sim 0.1 \mu\text{m}$)
- $10^{15}/\text{cm}^2$, 10 MeV Au (peak at 2.2 μm , FWHM $\sim 0.25 \mu\text{m}$).

The implantations have been performed at 500 °C, close to the temperature range boron carbide undergoes in a sodium fast neutron reactor. The flux ratio has been chosen to be close the He to dpa ratio we estimated here above, taking into account the accelerators requirements. The maximum He concentration is about $7.10^{20}/\text{cm}^3$. The total damage (Au + He) in the He implanted zone is about 1.2 dpa, the damage to He ratio is then about 200. After annealing at 1100 °C for one hour to allow the formation of helium clusters, transmission electron microscopy has been performed on samples prepared with FIB. The single beam implanted sample show a low density of parallel platelets in the implanted zone. The dual-beam implanted sample show a high

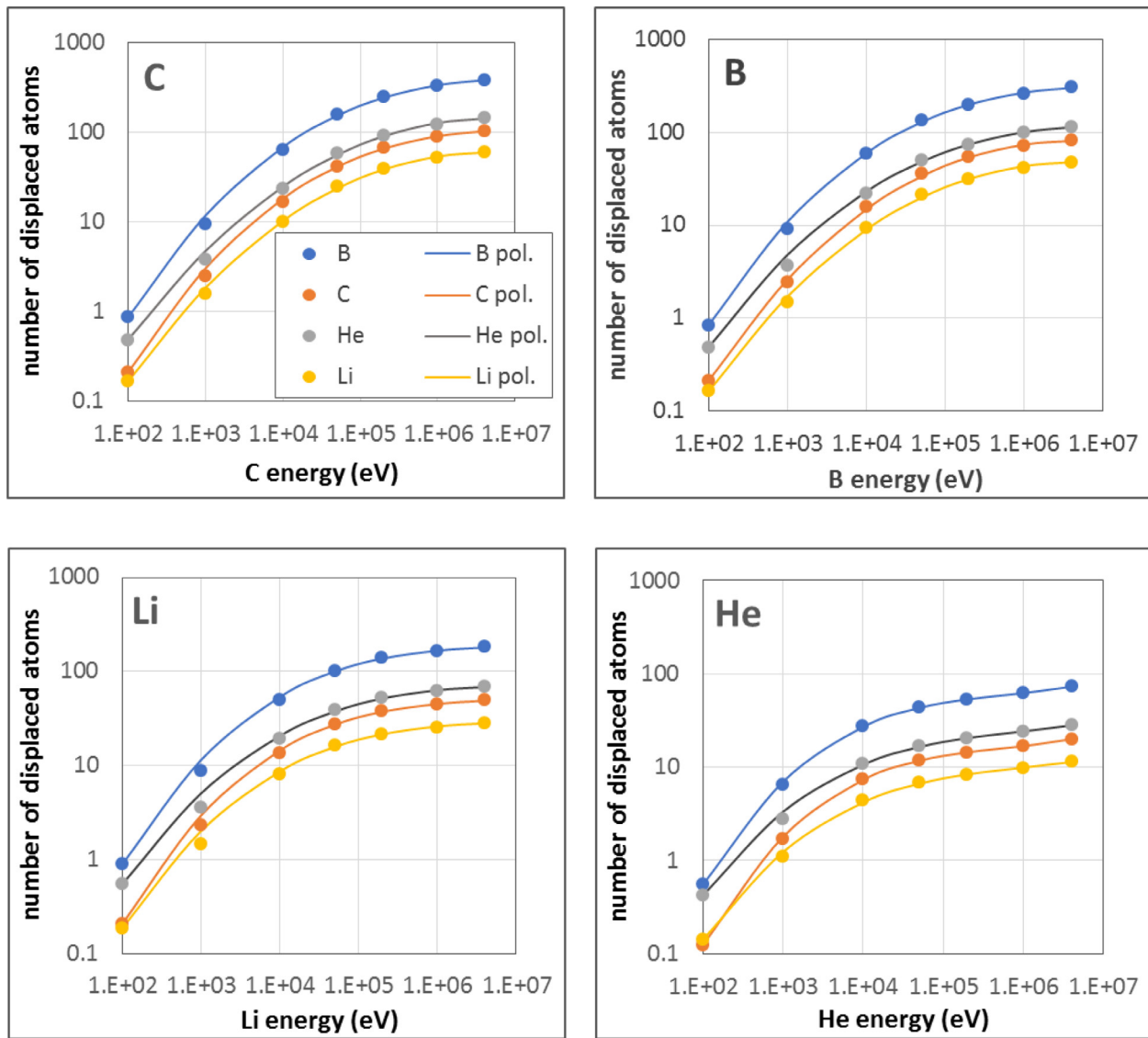


Fig. 10. Number of displaced atoms in B₄C (with burnup 10²².cm⁻³) per impinging atom (C, B, Li, He) as a function of the impinging atom energy as evaluated by SRIM. Dots: calculated values. Lines: polynomial fitting.

Table 2

Atom displacements rates (s⁻¹ × 10⁹) for an equivalent 'B₄C' atom irradiated in Phenix reactor, for a 10²².cm⁻³ burnup. With/without (n,α): taking into account or neglecting the contribution coming from the slowing-down of He and Li produced in the (n,α) reactions.

	B	C	He (10 ²² .cm ⁻³)	Li (10 ²² .cm ⁻³)
with (n,α)	973	252	365	150
without (n,α)	890	233	333	136

density of small bubbles (Fig. 11). Note they also both show bubbles in the grain boundaries. This clearly evidences the role of damage in the formation of the helium bubbles, this explaining the high density of bubbles observed after irradiation in reactors [23]. As mentioned above, helium mobility is much higher than the B and C ones, which stimulates the nucleation and growth of the clusters.

5. Conclusion

We have estimated the ratio of the number of displaced atoms to

Table 3

Main characteristics of some ion irradiations of B₄C boron carbide. Collision (density of displaced atoms), Se (electronic stopping power) and Sn (ballistic stopping power) are given at mid-range.

ion	Energy (MeV)	Range (μm)	Stragglng (μm)	Collision (at./Å)	Se (eV/Å)	Sn (eV/Å)
Au	1	0.188	0.023	2.5	440	350
	4	0.650	0.065	1.5	550	250
	10	1.67	0.16	0.8	550	160
Bi	0.8	0.155	0.017	2.8	400	300
	Ar	0.8	0.509	0.070	0.22	140
C	0.6	0.735	0.063	0.025	80	2
Fe	10	3.14	0.18	0.08	280	10
S	100	21.5	0.15	0.0015	500	0.15

helium production in boron carbide irradiated in a fast neutron spectrum. A value about 305 atom displacements per produced helium is obtained. Most of the energy of the displaced particles is dissipated via electronic processes, with stopping power Se lower than or around 150 eV/Å. Such results are to be used in order to simulate the behavior of helium produced in boron carbide. Dual-beam ion implantations can

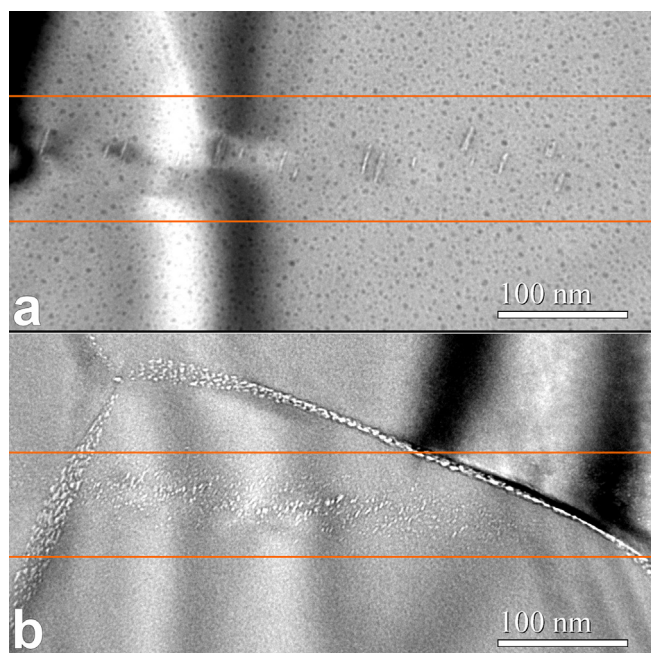


Fig. 11. Helium bubbles in irradiated boron carbide, from [20,21]. a: single He beam. b: dual He-Au beam. Bubbles also form in grain boundaries (orange lines: delimitation of the He implanted zone). (For interpretation of the references to colour in this figure legend, the reader is referred to the web version of this article.)

then be performed with He and a second ion, the role of which is creating a significant and representative damage. The calculation we performed here allowed choosing the right parameters of the irradiation, second ion nature, energies, relative fluence, allowing a realistic simulation of the damage to helium ratio. Preliminary TEM observations of a dual-beam irradiated sample show helium clusters distribution is similar to those observed after fast neutron irradiation, quite different from those resulting from a single He implantation.

Acknowledgements

This study was supported by the CEA-CNRS NEEDS-MATERIAUX collaborative research group. We are very indebted to the JANNUS-Saclay team for performing the dual-beam implantations.

References

- [1] G.S. Was, Z. Jiao, E. Getto, K. Sun, A.M. Monterrosa, S.A. Maloy, O. Anderoglu, B.H. Sencer, M. Hackett, Emulation of reactor irradiation damage using ion beams, *Scr. Mater.* 88 (2014) 33–36.
- [2] S.J. Zinkle, S. Kojima, Helium-assisted cavity formation in ion-irradiated ceramics, *J. Nucl. Mater.* 179–181 (1991) 395–398.
- [3] W. Wesch, E. Wendler (Eds.), *Ion Beam Modification of Solids*, Springer, 2016.
- [4] K. Yasuda, C. Kinoshita, S. Matsumura, Effects of simultaneous displacive and ionizing radiation in ionic and covalent crystals, *Defect Diffus. Forum* 206–207 (2002) 53–74.
- [5] D. Gosset, Absorber materials for Gen-IV reactors, in: P. Yvon (Ed.), *Structural Materials for Generation IV Nuclear Reactors*, Elsevier, 2017Ch. 15.
- [6] J.F. Ziegler, J.P. Biersack, M.D. Ziegler, SRIM, The Stopping and Range of Ions in Matter, <http://www.srim.org/>.
- [7] R. E. Stoller, K. Nordlund, S.P. Simakov, Summary Report of the Technical Meeting on Primary Radiation Damage: from nuclear reaction to point defects, IAEA reports, INDC(NDS)-0624, 2012.
- [8] L. Lunéville, D. Simeone, C. Jouanne, Calculation of radiation damage induced by neutrons in compound materials, *J. Nucl. Mater.* 353 (2006) 89–100.
- [9] R.E. Stoller, M.B. Toloczko, G.S. Was, A.G. Certain, S. Dwaraknath, F.A. Garner, On the use of SRIM for computing radiation damage exposure, *Nucl. Instrum. Methods B* 310 (2013) 75–80.
- [10] P. Filliatre, C. Jammes, B. Geslot, L. Buiron, In vessel neutron instrumentation for sodium-cooled fast reactors: type, lifetime and location, *Ann. Nucl. Energy* 37 (2010) 1435–1442.
- [11] Evaluated Nuclear Data File (ENDF) Database, Version of 2017-06-01, <https://www-nds.iaea.org/exfor/endl.htm>.
- [12] T.A. Ivanova, et al., Cross-section of the Production of Tritium in Interactions of Neutrons with ^{10}B Nuclei, *Phys. Part. Nucl. Lett.* 10–4 (2013) 353–356.
- [13] L. Zuppiroli, R. Kormann, D. Lesueur, Etude fondamentale du carbure de bore industriel, CEA report CEA-R-5237, 1983.
- [14] V. Motte, D. Gosset, T. Sauvage, H. Lecoq, N. Moncoffre, Evaluation of the diffusion coefficient of helium in implanted boron carbide by a NRA method, to be published.
- [15] H. Tsuchihir, T. Oda, S. Tanaka, Molecular-dynamics simulation of threshold displacement energies in lithium aluminate, *Nucl. Instrum. Methods -B* 269–14 (2011) 1707–1711.
- [16] H. Kinchin, R.S. Pease, The displacement of atoms in solids by radiation, *Rep. Progr. Phys.* 18 (1955) 1–51.
- [17] M.J. Norgett, M.T. Robinson, I.M. Torrens, A proposed method of calculating displacement dose rates, *Nucl. Eng. Des.* 33 (1975) 50–54.
- [18] L. Thomé, et al., Radiation effects in nuclear materials: role of nuclear and electronic energy losses and their synergy, *Nucl. Instrum. Methods B* 307 (2013) 43–48.
- [19] G. Victor, Y. Pipon, N. Béret, N. Toulhoat, N. Moncoffre, N. Djourelou, S. Miro, J. Baillet, N. Pradeilles, O. Rapaud, A. Maître, D. Gosset, Structural modifications induced by ion irradiation and temperature in boron carbide B4C, *Nucl. Instrum. Methods-B* 365 (2015) 30–34.
- [20] V. Motte, Helium behaviour in implanted boron carbide, thesis University Lyon-1 (France), 08-11-2017.
- [21] V. Motte, D. Gosset, N. Moncoffre, G. Gutierrez, Helium cluster nucleation and growth in implanted B4C boron carbide, to be published.
- [22] S. Pellegrino, P. Trocellier, S. Miro, Y. Serruys, É. Bordas, H. Martin, N. Chaâbane, S. Vaubaillon, J.P. Gallien, L. Beck, The JANNUS Saclay facility: a new platform for materials irradiation, implantation and ion beam analysis, *Nucl. Instrum. Methods-B* 273 (2012) 213–217.
- [23] T. Stoto, N. Housseau, L. Zuppiroli, B. Kryger, Swelling and microcracking of boron carbide subjected to fast neutron irradiations, *J. Appl. Phys.* 68–7 (1990) 3198.